Article:
Elworthy, S., Savage, A.M., Wilkinson, R.N. et al. (2019) The role of endothelial cilia in post-embryonic vascular development. Developmental Dynamics, 248 (6). pp. 410-425. ISSN: 1058-8388

https://doi.org/10.1002/dvdy.40

The role of endothelial cilia in post-embryonic vascular development

Stone Elworthy[1], Aaron M. Savage[1], Robert N. Wilkinson[1], Jarema J. Malicki[2]*, Timothy J. A. Chico[1]*.

[1]The Bateson Centre & Department of Infection, Immunity & Cardiovascular Disease, University of Sheffield

[2]The Bateson Centre & Department of Biomedical Science, University of Sheffield

University of Sheffield Medical School, Beech Hill Road, Sheffield, S10 2RX, United Kingdom

* joint senior authors

e-mail: t.j.chico@sheffield.ac.uk

Telephone +44 114 222 2396

Keywords

Zebrafish, elipsa, cilia, angiogenesis, vascular development, vascular mural cells

Running title

Cilia and zebrafish vascular development

Grant Sponsor and Grant Number

British Heart Foundation Infrastructure Award IG/15/31328 to TC, British Heart Foundation Project Grant PG/15/17/31332 to TC and JM, Medical Research Council MR/N000714/1to JM

Reviewers to exclude:

Didier Stanier (Max Planck), Julien Vermot (Strasbourg), Massimo Santoro (Belgium)

Abstract

Background

Cilia are essential for morphogenesis and maintenance of many tissues. Loss-of-function of cilia in early zebrafish development causes a range of vascular defects including cerebral haemorrhage and reduced arterial vascular mural cell coverage. In contrast, loss of endothelial cilia in mice has little effect on vascular development. We therefore used a conditional rescue approach to induce endothelial cilia ablation after early embryonic development and examined the effect on vascular development and mural cell development in post-embryonic, juvenile and adult zebrafish.

Results

ift54(elipsa) mutant zebrafish are unable to form cilia. We rescued cilia formation and ameliorated the phenotype of *ift54* mutants using a novel *Tg(ubi:loxP-ift54-loxP-myr-mcherry,myl7:EGFP)sh488* transgene expressing wildtype *ift54* flanked by recombinase sites, then used a *Tg(kdrl:cre)s898* transgene to induce endothelial-specific inactivation of *ift54* at post-embryonic ages. Fish without endothelial *ift54* function could survive to adulthood and exhibited no vascular defects. Endothelial inactivation of *ift54* did not affect development of *tagln*-positive vascular mural cells around either the aorta or the caudal fin vessels, nor formation of vessels after tailfin resection in adult animals.

Conclusions

Endothelial cilia are not essential for development and remodelling of the vasculature in juvenile and adult zebrafish when inactivated after embryogenesis.

Introduction

Cilia are cellular protrusions that play diverse roles in many different cell types. In vertebrates, cilia detect and process extracellular signals including light, chemicals, growth factors, morphogens, and mechanosensory stimuli (Goetz and Anderson, 2010; Malicki and Avidor-Reiss, 2014; Nachury, 2014; Malicki and Johnson, 2017). Mutations of vertebrate ciliary genes result in severe embryonic abnormalities including aberrant left-right asymmetry, defective dorso-ventral patterning of the spinal cord, failure of neural tube closure, and polydactyly (Goetz and Anderson, 2010). At later stages of development and in adult life, ciliary defects result in kidney and liver cyst formation, photoreceptor degeneration, obesity, anosmia, and mental retardation (Oh and Katsanis, 2012; Reiter and Leroux, 2017). In zebrafish, cilia mutants display a characteristic curved shape of the body axis, cystic kidney, and photoreceptor degeneration (Sun et al., 2004; Tsujikawa and Malicki, 2004; Kramer-Zucker et al., 2005; Zhao et al., 2012; Pooranachandran and Malicki, 2016). These phenotypes correlate well with the clinical features of human ciliopathies.

Correct development and homeostasis of the vertebrate vasculature requires mechanosensation of blood flow and the forces it exerts on the vessel, particularly shear stress (Jones et al., 2006; Potente et al., 2011; Baeyens et al., 2016). Endothelial cilia contribute to flow sensing in zebrafish at early development stages when blood flow has just commenced (Goetz et al., 2014). However, endothelial cilia are characteristically present at regions of low shear while higher shear leads to disassembly and loss of endothelial cilia (Iomini et al., 2004; Goetz et al., 2014).

Several zebrafish studies have shown a role for cilia in early vascular development. Localized morpholino knockdown of cilia at the age when blood flow first commences leads to abnormal caudal vein remodelling (Goetz et al., 2014). Zebrafish *iguana* and *MZtalpid3* mutants lack cilia from the earliest developmental stages and display intracranial haemorrhage (Lamont et al., 2010; Ben et al., 2011). which in *iguana* mutants is an indirect consequence of dysregulated Hedgehog pathway signalling. Hedgehog signalling induces *angiopoetin1* expression in mesenchymal cells which is required for vascular integrity (Lamont et al., 2010). Moreover, embryos that lose cilia after early embryogenesis due to mutations in the IFT-B complex genes *ift81*, *ift172*, and *qilin* also have high rates of intracranial haemorrhage (Kallakuri et al., 2015). Pharmacological and combined transient transgenic and morpholino approaches suggested that vascular integrity depends directly on endothelial cilia and Hedgehog signalling (Kallakuri et al., 2015). During vessel maturation, non-endothelial vascular mural cells are recruited to blood vessels (Santoro et al., 2009). Chen *et al.* used pharmacological and transient transgene-delivered CRISPR to show that endothelial cilia are also required for mural cell recruitment to developing arteries early in development (Chen et al., 2017).

In contrast to these severe effects of cilia depletion reported in zebrafish embryos, murine conditional knockout studies revealed a more subtle requirement for cilia in vascular development. Endothelial ablation of either cilia or the hedgehog pathway component Smo from the earliest developmental stages does not prevent mice from developing to healthy adulthood, although with an increased susceptibility to atherosclerosis (Dinsmore and Reiter, 2016). Lack of endothelial cilia caused a delay

in retinal vessel remodelling but by adulthood mice had no apparent vascular defects (Vion et al., 2018).

The observation that lack of cilia early in development leads to severe vascular defects in zebrafish, but mild or no defects in mice, coupled with the observation that vascular abnormalities are rarely associated with human ciliopathies, led us to ask what effect loss of cilia has in zebrafish after the initial phases of embryonic vascular development (vasculogenesis and sprouting angiogenesis). To test this, we developed a conditional rescue approach that inactivates cilia specifically in the endothelial cells of zebrafish after the early stages of development. We used this to examine the effect of endothelial cilia ablation on vascular development and mural cell recruitment in post-embryonic, juvenile and adult zebrafish and in regenerating tissue in adults.

Results

Transgenic partial rescue of *ift54*^{tp49} mutants

Absence of intraflagellar transport (IFT) genes leads to loss of cilia in all species examined, from Tetrahymena to mammals (Brown et al., 1999; Pazour et al., 2000; Han et al., 2003; Tsujikawa and Malicki, 2004). The zebrafish *ift54(elipsa)* locus encodes IFT54, an essential component of the IFT particle (Omori et al., 2008), and *ift54* loss-of-function leads to absent cilia. Zebrafish *ift54* mutants, such as the *ift54*^{tp49} allele used in this study, develop a severe body curvature (referred to as "curly-down") typical of cilia defects (Malicki et al., 1996; Omori et al., 2008). In addition, *ift54* mutants display kidney cysts, photoreceptor degeneration, peritoneal oedema, and die by 5-7 dpf (days postfertization). As these lethal defects preclude

analysis of cilia function later in life, we sought to develop a strategy that would rescue the early lethality of global *ift54* mutation and inactivate *ift54* specifically in endothelial cells, to test the requirement for cilia in post-embryonic vascular development and maintenance.

Injection of *ift54* mRNA has been shown to transiently rescue the phenotype of *ift54*^{tp49} mutants (Omori et al., 2008). This prompted us to attempt long-term rescue using a conditional stable transgene. We thus generated a *ubi:loxP-ift54-loxP-myr-mcherry,myl7:EGFP* construct (**Figure 1A**) that uses the ubiquitous *ubi* promoter (Mosimann et al., 2011) to drive expression of wild-type *ift54* flanked by loxP sites. The construct also includes a *myl7:egfp* cassette driving cardiac EGFP expression to facilitate identification of embryos expressing the transgene (Huang et al., 2003b). We generated a stable transgenic line that transmitted *myl7:egfp* to 50% of its progeny, indicating a single transgenic insertion. This is designated *Tg(ubi:loxP-ift54-loxP-myr-mcherry,myl7:EGFP)sh488*, but for brevity we hereafter refer to it as *ubi:ift54*.

Crossing *ift54*$^{tp49/+}$; *ubi:ift54* with *ift54*$^{tp49/+}$ fish allowed us to compare *ubi:ift54* transgenic and non-transgenic siblings in both wildtype and *ift54* mutant backgrounds (**Figure 1B and 1C**). As expected, approximately 75% of embryos without the *ubi:ift54* transgene (distinguished by lack of EGFP expression in the heart) generated in such crosses were wild-type, while approximately 25% displayed the characteristic curly-down *ift54*^{tp49} phenotype. Of embryos with the *ubi:ift54* transgene, approximately 75% were wild-type in appearance, showing that *ift54* overexpression by the transgene does not perturb normal development (**Figure 1B**). The remaining

25% of embryos with the *ubi:ift54* transgene showed a range of abnormalities from the typical curly-down phenotype to almost completely rescued but with a minor alteration in body axis (**Figure 1B**). The penetrance of the rescue by the *ubi:ift54* transgene varied widely between clutches **(Figure 1C)**.

Although not all homozygous *ift54*^{tp49} mutants were rescued by the *ubi:ift54* rescue transgene some survived to adulthood (**Figure 1D**). These rescued *ift54*^{tp49} mutant adults displayed a scoliosis similar to that seen in zebrafish mutants of *ptk7* and *c21orf59* (Grimes et al., 2016) but no other adverse effects were observed.

Cre-mediated recombination inactivates the *ubi:ift54* rescue transgene and induces mCherry expression.

As the wild-type *ift54* coding sequence in the *ubi:ift54* construct is flanked by loxP sites, Cre-mediated recombination should both excise the *ift54* transgene and induce expression of mCherry (**Figure 2A**). To test this was successful we examined the phenotypes of *ubi:ift54* transgenic and non-transgenic embryos from the same clutches injected with or without cre mRNA .

As expected, embryos without the *ubi:ift54* rescue transgene were either wild-type or developed the typical *ift54*^{tp49} curly-down phenotype in the expected 3:1 Mendelian ratio and *cre* injection did not affect this (**Figure 2B, first and third columns**). Consistent with the data in figure 1, of embryos carrying the *ubi:ift54* rescue transgene there was a marked reduction in the proportion of embryos displaying the curly-down phenotype (**Figure 2B, second column and Figure 2C**). Injection of *cre* abolished this ability of the *ubi:ift54* rescue transgene to prevent the curly-down

phenotype (**Figure 2B, fourth column and Figure 2C**). When we examined these embryos for mCherry expression, we found that *cre* injection induced global mCherry expression in embryos carrying the *ubi:ift54* transgene (**Figure 2C**) since the mRNA injection was not targeted to any organ or tissue.

The ubi:ift54 transgene partially rescues cilia formation in *ift54* mutants and is inactivated by Cre-mediated recombination

ift54^{tp49} mutants lack cilia in cristae, neuromasts, the nasal pit, and other tissues at 4dpf (Omori et al., 2008). We examined whether the *ubi:ift54* transgene rescues cilia formation. To this end, we performed acetylated tubulin staining to visualise cilia in wild-types, *ift54*^{tp49} mutants with or without the *ubi:ift54* rescue transgene, and *ift54*^{tp49} mutants with the *ubi:ift54* rescue transgene inactivated by *cre* mRNA injection. Fifty three preselected rescued *ift54*^{tp49}; *ubi:ift54* embryos were examined alongside 42 wt embryos, 25 *ift54*^{tp49} mutant embryos and 19 *cre* mRNA injected *ift54*^{tp49}; *ubi:ift54* embryos.

As expected, cilia were abolished in *ift54*^{tp49} mutants without the transgene (**Figure 3A**). However, the *ubi:ift54* transgene rescued cilia formation in homozygous *ift54*^{tp49} mutants in the cristae and neuromasts, but not in the nasal pit, consistent with our observation that the *ubi:ift54* transgene only partially rescues the effect of the *ift54*^{tp49} mutation. Recombination of the *ubi:ift54* transgene by Cre injection prevented rescue of cilia by the transgene in the cristae or neuromasts.

Cilia are critical for renal homeostasis (Sun et al., 2004; Drummond, 2009) and *ift54*^{tp49} mutants do not survive the early stages of life. Although the *ubi:ift54* transgene only partially rescues cilia formation, it does allow some homozygous *ift54*^{tp49} mutants to survive to adulthood, indicating that adequate cilia are maintained

for essential organ functions in these animals. We therefore examined the cilia of the pronephros in 13 dpf wild-type or *ift54^{tp49}; ubi:ift54* animals (*ift54^{tp49}* mutants without rescue do not survive to this stage so could not be examined). We found that pronephric cilia formation was preserved in *ift54^{tp49}; ubi:ift54* animals (**Figure 3B**), consistent with their ability to survive into adulthood.

Endothelial-specific inactivation of the *ubi:ift54* transgene

To test the role of cilia in the vasculature, we sought to inactivate the *ubi:ift54* rescue transgene specifically in endothelial cells. We generated homozygous *ift54^{tp49}* mutants rescued by *ubi:ift54* transgene and used a *Tg(kdrl:cre)s898* transgene (Bertrand et al., 2010) that expresses Cre in endothelial cells to inactivate the *ubi:ift54* rescue transgene. In addition, endothelial cells were visualised using a *Tg(fli1a:LIFEACT-clover)sh467* transgene. We found that endothelial-specific mcherry expression was detectable at 7dpf (**Figure 4A**) and more pronounced at 10dpf (**Figure 4B**) indicating successful recombination and inactivation of the *ubi:ift54* rescue transgene by 10dpf. *ift54^{tp49}*; *ubi:ift54* siblings without *Tg(kdrl:cre)s898* lacked mcherry expression as expected, thus providing a control group that allowed us to test the effect of ablation of endothelial cilia on patterning and morphology of blood vessels in juvenile and mature animals.

The effect of inactivation of endothelial on vascular development

We first used a *Tg(fli1a:LIFEACT-clover)sh467* transgenic line to examine the vascular networks in rescued *ift54^{tp49}*; *ubi:ift54* fish with and without endothelial specific inactivation of the rescue transgene compared with wild types. **Figure 5A** shows the entire vascular anatomy of representative 10 dpf wild type, *ift54^{tp49}*;

ubi:ift54 and *ift54*^{tp49}; *ubi:ift54; Tg(kdrl:cre)s898* zebrafish. *Tg(kdrl:cre)s898* mediated recombination did not result in any changes in vascular patterning that we could detect. The *Tg(fli1a:LIFEACT-clover)sh467* and *Tg(fli1a:EGFP)y1* transgenes both label endothelial cells but differ as to which allows higher resolution analysis depending upon tissue and stage of development. We used the *Tg(fli1a:EGFP)y1* transgene to visualise endothelial cells of the cerebral vasculature. This revealed no effect of endothelial-specific recombination of the rescue transgene (**Figure 5B**) although this stage of development may be too soon after recombination to detect an effect, especially since a significant proportion of the trunk and cerebral vasculature develops early (2-5 dpf), possibly before we achieved endothelial-specific cilia ablation. This raises the possibility that cilia are required for initial vessel formation but not for subsequent maintenance, growth or remodelling. We therefore examined the effect of endothelial cilia ablation on formation of vascular beds that form after 10 dpf (the stage at which we had confirmed Cre-mediated recombination of the rescue transgene). Between 9 dpf and 14 dpf, the caudal fin undergoes metamorphosis (Parichy et al., 2009) and differentiates a vascular bed that initially forms as a mesh-like plexus that remodels into radial arteries and veins (**Figure 6A**). As elsewhere in the vasculature of 10 dpf *ubi:ift54; Tg(kdrl:cre)s898* animals, the vessels of the developing caudal fin expressed mcherry (**Figure 6A**, see also **Figure 11**); confirming the rescue transgene had undergone Cre-mediated recombination to inactivate *ift54*.

We next used the *Tg(fli1a:LIFEACT-clover)sh467* transgene to compare the structures of 14 dpf caudal fin vascular networks of rescued *ift54*^{tp49}; *ubi:ift54* fish with and without endothelial-specific recombination of the rescue transgene (**Figure 6B**).

Endothelial-specific recombination of the rescue transgene caused no apparent further defect to the vessel bed of partially rescued fish compared with rescued *ift54* mutants.

We then examined caudal fin vascular beds at 13 dpf when they were undergoing a highly active stage of growth and remodelling. At this stage too, examination of the caudal fin vascular beds of rescued *ift54*^{tp49}; *ubi:ift54* fish with and without endothelial specific recombination of the rescue transgene did not reveal any requirement for endothelial cilia (**Figure 6C**). The variable pattern and size of the vascular beds between individual *ift54*^{tp49}; *ubi:ift54* fish (**Figure 6C**) reduces the statistical power to detect small differences. However, these group sizes were sufficient to exclude a profound effect on vascular development in this vascular bed induced by cilia ablation.

We attempted to determine whether the vessels of the developing caudal fin possess endothelial cilia. We performed acetylated tubulin immunostaining to visualise cilia together with the *Tg(fli1a:LIFEACT-clover)sh467* transgene that labels endothelial cells. We examined wild-types and compared these with *ift54*^{tp49} mutants partially rescued by the *ubi:ift54* rescue transgene, and with *ift54*^{tp49}*; ubi:ift54* partially rescued mutants with *Tg(kdrl:cre)s898* to induce endothelial recombination as in earlier studies. To correct for the developmental delay observed in the mutants, wild-types were examined at 11 dpf whilst the slower developing rescued mutants were examined at 13 dpf. *Tg(fli1a:LIFEACT-clover)sh467* expressing endothelial cells were visualised by anti-GFP staining and auto-fluorescence of erythrocytes allowed identification of vessel lumens. We identified occasional putative endothelial cilia protruding into vessel lumens in wild-types and in partially rescued mutants that had the unrecombined rescue transgene but not in partially rescued mutants with

endothelial recombination (**Figure 7**). Cilia on adjacent cells were observed in all three genotypes (**Figure 7**). However, the low number of putative endothelial cilia in wildtypes and the difficulty in confirming these to be endothelial in origin makes us cautious about interpreting this data.

Examination of the adult vasculature with endothelial specific excision of the rescue transgene

We raised rescued sibling *ift54*^{tp49}; *ubi:ift54* fish with and without endothelial cilia ablation by *Tg(kdrl:cre)s898* to adulthood. Both groups display scoliosis consistent with the partial extent of the rescue and the role of cilia in spinal development. However, there was no apparent worsening of the severity of the phenotype caused by endothelial cilia ablation (**Figure 8A**). We examined vascular patterning in various tissues in these adult fish and their wild-type siblings using *Tg(fli1a:EGFP)y1* to visualize blood vessels. The vasculature of the swim bladder posterior chamber and the pectoral fin appeared no different between wild-type, rescued *ift54*^{tp49}; *ubi:ift54* animals, or *ift54*^{tp49}; *ubi:ift54; Tg(kdrl:cre)s898* fish without endothelial cilia (**Figure 8B**).

To test the role of endothelial cilia in formation of blood vessels in regenerating tissue in adults (weeks after the age at which we had confirmed inactivation of the rescue transgene in endothelial cells) we amputated the caudal fin of adult fish and examined the vasculature in the regenerated fin four days post amputation. This revealed no difference in vascular patterning in the regenerated fin between wild-types, rescued *ift54* mutants, and rescued *ift54* mutants with endothelial cilia ablation (**Figure 8B**).

We next examined the adult retinal vasculature. We observed that compared with wild-types, the retinal vasculature of partially rescued *ift54*^{tp49}; *ubi:ift54* animals appeared to exhibit an increase in small branches and sprouts in the peripheral retinal vessels. However although we observed a similar appearance in the retinal vessels of animals with endothelial cilia ablation mediated by *Tg(kdrl:cre)s898* this was no worse than in rescued *ift54*^{tp49}; *ubi:ift54* animals (**Figure 9**).

The role of endothelial cilia in vascular mural cell recruitment.

Ablation of endothelial cilia early in development has been reported to prevent recruitment of vascular mural cells to the aorta at 3 dpf (Chen et al., 2017). We therefore examined the effect of ablation of endothelial cilia on vascular mural cells in older zebrafish. We used in situ hybridization for the mural cell marker *tagln* to examine partially rescued *ift54*^{tp49}; *ubi:ift54* fish with and without endothelial specific recombination of the rescue transgene (**Figure 10**). At 13 dpf, *tagln* expression is prominent around arteries such as the dorsal aorta in the trunk. We observed no difference in *tagln* expression between wild-type, rescued *ift54*^{tp49}; *ubi:ift54* animals, or *ift54*^{tp49}; *ubi:ift54; Tg(kdrl:cre)s898* fish with ablated endothelial cilia (**Figure 10A**). This suggests that endothelial cilia are not required for the maintenance of vascular mural cells.

The caudal fin vascular bed forms after the stage at which we observe Cre-mediated recombination of the rescue transgene in endothelial cells (**Figure 6**) (Parichy et al., 2009). In situ hybridisation showed similar levels of *tagln* expression in the caudal fin of partially rescued adult *ift54*^{tp49}; *ubi:ift54* fish with or without endothelial Cre mediated recombination from *Tg(kdrl:cre)s898* (**Figure 10B**).

To extend these studies we used a transgenic line *Tg(tagln:mcherry)sh441* to visualise mural cells in the caudal fin vascular bed soon after its formation *in vivo*. We were concerned that interpretation of the data from these animals might be confounded by simultaneous mcherry expression from our *ubi:ift54* rescue transgene after Cre mediated recombination. However, mcherry expression in mural cells from *Tg(tagln:mcherry)sh441* is considerably brighter than that in endothelial cells from our *ubi:ift54* rescue transgene after recombination (**Figure 11**). With the laser power required for detecting *Tg(tagln:mcherry)sh441*, endothelial mcherry expression from the recombined *ubi:ift54* transgene was insignificant (**Figure 11**). Examination of this *Tg(tagln:mcherry)sh441* transgenic allowed us to examine the effect of endothelial inactivation of *ift54* on mural cell coverage in the fin vascular bed. We observed similar levels of mural cell coverage in partially rescued, *ift54*^{tp49}; *ubi:ift54* 17 dpf fish with or without endothelial Cre mediated recombination from *Tg(kdrl:cre)s898.* This suggests perivascular mural cells can be recruited to vessels in the caudal fin despite inactivation of endothelial *ift54* (**Figure 12**).

Discussion

Endothelial cilia have been implicated in a range of developmental and pathological processes. The forces exerted by blood flow are necessary for embryonic vascular development and postnatal vascular health (Jones et al., 2006; Potente et al., 2011; Baeyens et al., 2016; Garcia-Cardena and Slegtenhorst, 2016). Since endothelial cilia sense such forces under certain conditions, they are plausible candidates for roles in these processes, although many other endothelial mechanosensitive pathways exist, such as the PECAM/VEGFR2 complex, integrins, the cytoskeleton, and channels such as Piezo1. Aside from their role in mechanosensation, cilia play

important roles in signalling pathways critical to embryonic vascular development, notably Hedgehog (Huangfu et al., 2003; Huang and Schier, 2009). Previous studies described cerebral haemorrhage in zebrafish embryos resulting from Hedgehog signalling defects due to loss of cilia in endothelial cells (Kallakuri et al., 2015) and in surrounding tissues (Lamont et al., 2010). However, in mice, elimination of Hedgehog signalling in endothelial cells from the earliest stages of their specification did not perturb vascular development (Dinsmore and Reiter, 2016).

Formation of mature blood vessels requires not only endothelial cells but recruitment of mural pericytes or vascular smooth muscle cells. Previous studies showed that ablation of endothelial cilia early in embryonic development reduced mural cell coverage of the dorsal aorta, implying that endothelial ciliary function signals to contribute to recruitment or differentiation of these cells (Chen et al., 2017).

Our work adds to the previous studies which examined the effect of loss of cilia early in development by showing that when endothelial cilia are ablated at post-embryonic ages, zebrafish can develop from larvae to adulthood without evidence of abnormal vascular development. Prior to examining vascular development we confirmed that a) cilia formation in *ift54* mutants is largely restored by our floxed *ift54* rescue transgene, b) this greatly ameliorates the *ift54* phenotype c) cre-mediated recombination abolishes the effect of the rescue transgene and restores the *ift54* mutant phenotype d) endothelial-specific Cre expression driven by the endothelial-specific *kdrl* promoter successfully induced recombination of the rescue transgene in the vasculature. These findings make us confident that following endothelial recombination, endothelial cilia formation would have been prevented.

Despite inactivation of the rescue transgene and hence inactivation of *ift54* in endothelial cells from 10dpf, we observed no defects in endothelial patterning in any

of the vascular beds we observed (trunk, brain, swim bladder, normal or regenerating caudal fin). Although we observed subtle alterations in the peripheral retinal vessels of rescued *ift54* mutants, these were no more pronounced in animals with inactivation of the rescue transgene in endothelial cells, implying they arise as a result of imperfect rescue of cilia in non-endothelial cells. This finding of minor differences in retinal vessel patterning in response to subtle alterations in cilia function is interesting and warrants further study to determine which cell types are responsible and whether our rescued adult fish might allow insights into the retinopathy seen in humans with ciliopathy.

Our work does have some limitations. Firstly, we cannot exclude the possibility that inactivation of endothelial cilia induced subtle defects of vascular development that we were unable to detect and that will be uncovered by future, more detailed analyses. However, we can be confident that the major vessels imaged in our study were present and able to either form, or at least be maintained, in the absence of endothelial *ift54*. Secondly, our attempts at quantification of endothelial cilia by acetylated tubulin staining were limited by the difficulty of discriminating these from non-endothelial cilia. Although transgenic reporters that label the cilia have been generated, these similarly label all cilia, and are not specific to the endothelium (Borovina et al., 2010; Eisa-Beygi et al., 2018). For future work, an endothelial specific, cilia localising fluorescent transgene would be advantageous although combining this with the *kdrl:cre; ubi:ift54; ift54-/-; kdrl:mcherry* fish described in our study (ie six separate transgenic insertions or mutant alleles) would be technically demanding.

An important finding of our study is that vascular mural cells (VMC) were maintained around the aorta once endothelial cilia had been inactivated, and that vascular mural cells in the caudal fin were recruited to the caudal fin vessels even when these vessels do not form until after the point at which we had inactivated endothelial *ift54*. A previous study found that endothelial inactivation of *ift88* prevented VMC recruitment to the aorta at 80dpf (Chen et al., 2017). The same study showed that Notch signalling, known to be required for formation of the aorta by vasculogenesis (Lawson and Weinstein, 2002), is also required for VMC coverage. Our data suggests that different mechanisms govern VMC coverage of vessels that form later in development such as the caudal fin vessels. The reasons for such differences remain unclear but may relate to a lower requirement for Notch signalling in post-embryonic vascular development.

Generating tissue-specific mutations in zebrafish such as the one we describe here is still very challenging. Alternative strategies are being developed and may offer advantages over the conditional rescue approach we used. Another zebrafish study relied on a similar approach but used a BAC transgene and achieved a more complete conditional rescue (Liu et al., 2017). Knock-in based approaches to generating conditional mutant alleles appear even more promising than the conditional rescue approach we applied (Hoshijima et al., 2016; Sugimoto et al., 2017).

Although the rescue of *ift54* mutant phenotype in this study was incomplete, most *ift54* functions were restored by the conditional transgene used and in contrast to

ift54^{tp49} homozygotes, which are extremely abnormal by 5 dpf and die shortly thereafter (Malicki et al., 1996; Omori et al., 2008), some transgenic *ift54*^{tp49} homozygotes survive over a year. The zebrafish nose features non-motile cilia that project from multiciliated dendritic knobs of olfactory sensory neurons and motile cilia that differentiate from multicilated cells at the rim of the olfactory pit (Leventea et al., 2016; Reiten et al., 2017). The poor rescue of the nasal cilia suggest that multiciliated cells may be especially difficult to rescue as both type of cilia were poorly rescued in by our transgenic approach. Similarly, the scoliosis that we observe in rescued *ift54* mutant animals may due to defects in multiciliated ependymal cells, since defects in ependymal cell cilia have been shown to cause scoliosis (Grimes et al., 2016). It is possible that multiciliated cells require particularly high levels of IFT protein expression, including *ift54,* that were not achieved using the ubiquitous promoter on which our rescue transgene relied. Nevertheless, the *ift54*^{tp49}; *ubi:ift54* system we here describe represents a useful tool that could be applied to test the role of cilia in many organs and tissues, needing only appropriate *cre* driver lines.

Acknowledgements.

We are very grateful to the aquarium staff of the Bateson Centre for expert husbandry and advice.

Materials and Methods

Zebrafish strains and maintenance

Zebrafish were maintained in accordance with UK Home Office regulations and the UK Animals (Scientific Procedures) Act 1986. The *mitfa*^{w2} melanophore deficiency was used to facilitate imaging (Lister et al., 1999). *ift54*^{tp49} (Omori et al., 2008), *Tg(fli1a:EGFP)y1* (Lawson and Weinstein, 2002) and *Tg(kdrl:cre)s898* (Bertrand et al., 2010) have been previously described.

Construction of *Tg(ubi:loxP-ift54-loxP-myr-mcherry,myl7:EGFP)sh488*

The Tol2kit multisite gateway method (Kwan et al., 2007) was used with a *ubi* promoter 5'-entry plasmid (Mosimann et al., 2011), an *ift54*-loxP middle-entry plasmid, a loxP-2myr-mcherry 3'-entry plasmid and pDestTol2CG/pDestTol2CG2 vector (Kwan et al., 2007). The *ift54*-loxP middle-entry plasmid incorporated the *ift54* cDNA from (Omori et al., 2008) and oligonucleotide sequence (IDT) using standard PCR cloning methods. The loxP-2myr-mcherry 3'-entry plasmid was modified from p3E-mcherrypA (Kwan et al., 2007) with oligonucleotides (IDT) using standard PCR cloning methods. DNA sequencing confirmed the full transgene plasmid sequence (Core Genomics Facility University of Sheffield). The transgene plasmid was coinjected with tol2 transposase mRNA into zebrafish embryos from *ift54*$^{tp49/+}$ incrosses following standard methods (Kwan et al., 2007); embryos with heart EGFP were raised and outcrossed against *ift54*$^{tp49/+}$.

Generation of *Tg(tagln:mcherry)sh441*

Tg(tagln:mcherry)sh441 was generated using the Tol2kit multisite gateway method as above, using the following components, p5EtaglnECR5 (Seiler et al., 2010) (a kind

gift of Christoph Seiler and Michael Pack), pME-mCherry (Kwan et al., 2007) p3E-SV40pA (Kwan et al., 2007)pDestTol2pA2 (Kwan et al., 2007)

Generation of *Tg(fli1a:LifeAct-mClover)sh467*

Tg(fli1a:LifeAct-mClover)sh467 was similarly generated using the Tol2kit multisite gateway method by fusing the LifeAct F-actin binding motif (Riedl et al., 2008) to the N-terminus of mClover by PCR (Savage et al., 2019)

Zebrafish PCR genotyping

PCR genotyping for *ift54*^{tp49} used primers 5'-TGGTTATCATTTGTCTGTGTGGA-3' and 5'-GCTCTCTTTCTCGGCCTTTG-3' and then Sanger sequencing with primer 5'-TGGTTATCATTTGTCTGTGTGGA-3'. *Tg(kdrl:cre)s898* identification used PCR with primers 5'-CCCGGCAAAACAGGTAGTTA-3' and 5'-CGTACTGACGGTGGGAGAAT-3'. Cre mediated recombination of *Tg(ubi:loxP-ift54-loxP-myr-mcherry,myl7:EGFP)sh488* was tested with a nested PCR with 20 cycles using primers 5'-GAATTCGACCCAAGTTTGTACAA-3' and 5'-CATGTTATCCTCCTCGCCCT-3', then 20 cycles using primers 5'-TTGTAAAACGACGGCCAGTG-3' and 5'-CTTGATACAACCCATGGCGG-3', giving a 189bp product after cre-lox excision of the *ift54* cassette.

Cre mRNA injection

mRNA was synthesised from pCS2-Cre.zf1 and injected into single cell stage zebrafish embryos following (Horstick et al., 2015).

Zebrafish live imaging

Live images used Tricaine anesthesia. Adults were imaged immersed in aquarium water and embryos and juveniles were mounted in 1% low gelling temperature agarose. Whole animal images used a Leica M165FC microscope with Leica DFC

310FX camera. SPIM imaging of the vasculature of juvenile zebrafish used a Zeiss Lightsheet Z.1. Live confocal imaging used an Olympus FV1200 microscope.

Fluorescent vascular imaging of fixed adult tissue

Euthanised, decapitated *Tg(fli1a:EGFP)y1* adults were fixed overnight in 4% PFA in PBS at 4^{o}C then washed into PBS. The dissected tissue was mounted in Fluoroshield (Sigma). Retina vasculature flat mounts followed (Wiggenhauser et al., 2017), swim bladder posterior chamber flat mounts followed (Robertson et al., 2007), regenerated caudal fin flat mounts followed (Huang et al., 2003a). Imaging used a Nikon A1 confocal microscope.

In situ hybridisation and Immunofluorescence

In situ hybridisation followed (Braissant, 1998) with 20μm cryo-sections, digoxigenin labelled antisense *tagln* RNA probe (Santoro et al., 2009) and alkaline phosphatase chromogenic development with BM-Purple (Sigma-Aldrich). Micrographs used a Leica M165 FC microscope with Leica DFC310FX camera.

Immunofluorescence of embryos followed (Leventea et al., 2016). Wholemount immunofluorescence of embryos was imaged with an Olympus FV1200 confocal microscope and cryo-section immunofluorescence with a Nikon A1 confocal microscope.

For wholemount immunofluorescence, juvenile tails were fixed in 2% trichloroacetic acid in PBS for three hours at room temperature and stored in methanol at -20^{o}C. After rehydration into PBS and permeabilization with 2% TritonX100 in PBS at 4^{o}C for three days, standard procedures were followed using rabbit anti-GFP (Torrey Pines) and anti-acetylated tubulin (6-11B-1). The caudal fins were flat mounted in Fluoroshield (Sigma) and imaged with a Zeiss LSM880 AiryScan confocal microscope.

Figure Legends

Figure 1) The *Tg(ubi:loxP-ift54-loxP-myr-mcherry,myl7:EGFP)sh488* rescue transgene provides partial rescue of homozygous *ift54^{tp49}* mutants. (A) Diagram of the *ubi:loxP-ift54-loxP-myr-mcherry,myl7:EGFP* transgene. **(B)** 5dpf siblings from an *ift54$^{tp49/+}$*;*Tg(ubi:loxP-ift54-loxP-myr-mcherry,myl7:EGFP)sh488* x *ift54$^{tp49/+}$* cross. Sequencing traces show the *ift54^{tp49}* C-to-T mutation genotype (asterisk denotes stop codon). Homozygous mutant *ift54^{tp49}* (*ift54-/-*) embryos without the transgene display the expected "curly-down" phenotype. The *Tg(ubi:loxP-ift54-loxP-mcherry,myl7:EGFP)sh488* transgene (*ubi:ift54*) does not affect normal development compared with wild type (wt) but rescues the phenotype of some *ift54^{tp49}* homozygotes **(C)** Proportion of phenotypes of the transgenic (**+**) and nontransgenic (**-**) embryos from six *ift54$^{tp49/+}$*;*Tg(ubi:loxP-ift54-loxP-myr-mcherry,myl7:EGFP)sh488$^{/+}$* x *ift54$^{tp49/+}$* crosses. Total number of embryos is shown above each column. The extent of rescue varied considerably between clutches. **(D)** Five-month-old adult fish alongside sequencing traces showing the *ift54^{tp49}* C-to-T mutation genotype. *ift54^{tp49}* mutants with the *Tg(ubi:loxP-ift54-loxP-myr-mcherry,myl7:EGFP)sh488* transgene (*ift54-;ubi:ift54*) can survive into adulthood but develop scoliosis.

Figure 2) The *Tg(ubi:loxP-ift54-loxP-myr-mcherry,myl7:EGFP)sh488* rescue transgene is recombined after *cre* mRNA injection which abolishes its ability to rescue homozygous *ift54^{tp49}* mutants. **(A)** Diagram of the rescue transgene with and without Cre. Cre-mediated recombination excises wildtype *ift54* and induces mcherry expression. **(B)** Phenotype frequencies in *Tg(ubi:loxP-ift54-loxP-myr-mcherry,myl7:EGFP)sh488* transgenic (**+**) and nontransgenic (**-**) embryos from a typical clutch of a *ift54$^{tp49/+}$*;*Tg(ubi:loxP-ift54-loxP-myr-mcherry,myl7:EGFP)sh488$^{/+}$* x

ift54$^{tp49/+}$ cross. Embryos were injected with *cre* mRNA (**+**) or uninjected (**-**). *cre* injection prevents transgenic rescue. **(C)** Brightfield (top) and fluorescent (bottom) micrographs of 5dpf *cre* mRNA injected and uninjected embryos from an *ift54*$^{tp49/+}$;*Tg(ubi:loxP-ift54-loxP-myr-mcherry,myl7:EGFP)sh488*$^{/+}$ x *ift54*$^{tp49/+}$ cross. Embryos with the rescue transgene express GFP in the heart. Cre-mediated recombination prevents rescue of the phenotype and induces mcherry expression.

Figure 3) The *Tg(ubi:loxP-ift54-loxP-myr-mcherry,myl7:EGFP)sh488* rescue transgene restores cilia in *ift54*^{tp49} mutants. (A) Confocal stack projections of the crista of the ear and neuromasts, and confocal slices of the nasal epithelium of 4dpf embryos. Acetylated tubulin immunofluorescence of cilia axonemes (Green), DAPI staining of DNA in blue. Arrows show cilia axonemes or the positions where they missing. Images shown are representative of all of the embryos examined of each group from *ift54*$^{tp4/+}$;*Tg(ubi:loxP-ift54-loxP-myr-mcherry,myl7:EGFP)sh488*$^{/+}$ x *ift54*$^{tp49/+}$ crosses with or without *cre* mRNA injection. The rescue transgene restores cilia formation in the crista and neuromasts but not nasal epithelium. **(B)** Confocal stack projections of transverse sections of trunk at 13dpf. Acetylated tubulin (Green) immuno-fluorescence showing cilia axonemes of the pronephric ducts (white arrows), phalloidin staining of Actin in red, DAPI staining of DNA in blue. Images representative of all of three *ift54*^{tp49}; *Tg(ubi:loxP-ift54-loxP-myr-mcherry,myl7:EGFP)sh488* fish (***ift54-/-;ubi:ift54***) and three wt sibs (**wt**) examined. The rescue transgene rescues cilia of pronephric ducts. **Scale bars** 20μm.

Figure 4) Endothelial-specific excision of the *Tg(ubi:loxP-ift54-loxP-myr-mcherry,myl7:EGFP)sh488* rescue transgene. (A) SPIM stack projections of lateral

views of the head of 7dfp *ift54*^{tp49}; *Tg(ubi:loxP-ift54-loxP-myr-mcherry,myl7:EGFP)sh488*$^{/+}$;*Tg(fli1a:LIFEACT-clover)sh467*$^{/+}$ (***ift54-/-; ubi:ift54; fli1:clover***) and *ift54*^{tp49}; *Tg(ubi:loxP-ift54-loxP-myr-mcherry,myl7:EGFP)sh488*$^{/+}$;*Tg(kdrl:cre)s898*$^{/+}$;*Tg(fli1a:LIFEACT-clover)sh467*$^{/+}$ (***itf54-/-; ubi:ift54; fli1:clover; kdrl:cre***) fish showing endothelial Clover and faint mcherry expression. The position of the eye is labelled for orientation. Endothelial specific, Cre mediated recombination of the *Tg(ubi:loxP-ift54-loxP-myr-mcherry,myl7:EGFP)sh488* transgene is marked by mcherry expression. **(B)** at 10dpf mcherry expression is more pronounced than at 7dpf.

Figure 5) Endothelial-specific ablation of cilia does not perturb trunk or cerebral vascular development by 10dpf (A) SPIM stack projections showing endothelial Clover expression in lateral views of the head, anterior trunk, posterior trunk and tails of 10dpf *Tg(ubi:loxP-ift54-loxP-myr-mcherry,myl7:EGFP)sh488*$^{/+}$;*Tg(fli1a:LIFEACT-clover)sh467*$^{/+}$ (**wt**) (n=9) and *ift54*^{tp49}; *Tg(ubi:loxP-ift54-loxP-myr-mcherry,myl7:EGFP)sh488*$^{/+}$;*Tg(fli1a:LIFEACT-clover)sh467*$^{/+}$ (***ift54-/-;ubi:ift54***) (n=9) and *ift54*^{tp49}; *Tg(ubi:loxP-ift54-loxP-myr-mcherry,myl7:EGFP)sh488*$^{/+}$;*Tg(kdrl:cre)s898*$^{/+}$;*Tg(fli1a:LIFEACT-clover)sh467*$^{/+}$ (***ift54-/-;ubi:ift54;kdrl:cre***) (n=4) Fish. **(B)** SPIM stack projections showing endothelial EGFP expression in dorsal views of the head of 10dpf *Tg(ubi:loxP-ift54-loxP-myr-mcherry,myl7:EGFP)sh488*$^{/+}$;*Tg(fli1a:EGFP)y1*$^{/+}$ (**wt**) (n=4) and *ift54*^{tp49}; *Tg(ubi:loxP-ift54-loxP-myr-mcherry,myl7:EGFP)sh488*$^{/+}$; *Tg(fli1a:EGFP)y1*$^{/+}$ (***ift54-/-;ubi:ift54***) (n=3) and *ift54*^{tp49}; *Tg(ubi:loxP-ift54-loxP-myr-mcherry,myl7:EGFP)sh488*$^{/+}$;*Tg(kdrl:cre)s898*$^{/+}$; *Tg(fli1a:EGFP)y1*$^{/+}$ (***ift54-/-;ubi:ift54;kdrl:cre***) fish (n=12).

Figure 6) Endothelial-specific excision of the *Tg(ubi:loxP-ift54-loxP-myr-mcherry,myl7:EGFP)sh488* transgene causes no apparent further impairment to secondary caudal fin vasculature in *ift54^{tp49}*; *Tg(ubi:loxP-ift54-loxP-myr-mcherry,myl7:EGFP)sh488* fish. (A) SPIM stack projections of endothelial cells marked with Clover expression in the caudal fin of 10dpf and 14dpf *Tg(ubi:loxP-ift54-loxP-myr-mcherry,myl7:EGFP)sh488$^{/+}$;Tg(kdrl:cre)s898$^{/+}$*;*Tg(fli1a:LIFEACT-clover)sh467$^{/+}$* fish, showing endothelial specific Clover and myr-mcherry expression. **(B)** SPIM stack projections of endothelial cells marked with Clover in the caudal fin of 14dpf *ift54^{tp49}*; *Tg(ubi:loxP-ift54-loxP-myr-mcherry,myl7:EGFP)sh488$^{/+}$* ;*Tg(fli1a:LIFEACT-clover)sh467$^{/+}$* (***ift54-/-; ubi:ift54***) and *ift54^{tp49}*; *Tg(ubi:loxP-ift54-loxP-myr-mcherry,myl7:EGFP)sh488$^{/+}$;Tg(kdrl:cre)s898$^{/+}$* ;*Tg(fli1a:LIFEACT-clover)sh467$^{/+}$* (***ift54-/-; ubi:ift54; kdrl:cre***). The secondary caudal fin vasculature forms in the absence of endothelial *ift54* function. **(C)** SPIM stack projections of endothelial cells marked with Clover in the caudal fin of 13dpf *ift54^{tp49}*; *Tg(ubi:loxP-ift54-loxP-myr-mcherry,myl7:EGFP)sh488$^{/+}$* ;*Tg(fli1a:LIFEACT-clover)sh467$^{/+}$* (***ift54-/-; ubi:ift54***) and *ift54^{tp49}*; *Tg(ubi:loxP-ift54-loxP-myr-mcherry,myl7:EGFP)sh488$^{/+}$;Tg(kdrl:cre)s898$^{/+}$* ;*Tg(fli1a:LIFEACT-clover)sh467$^{/+}$* (***ift54-/-; ubi:ift54; kdrl:cre***) fish. The *Tg(kdrl:cre)s898$^{/+}$* caused no apparent impairment to the developing fin vascular bed in the fish with partial transgenic rescue of *ift54^{tp49}*. Chart shows caudal fin vessel bed relative areas measured from SPIM images. Overlay shows median and interquartile range. Two-tailed Mann-Whitney test P=0.7223.

Figure 7) Endothelial cilia are present in the juvenile caudal fin vascular plexus. Immunofluorescence confocal slices of anti-acetylated tubulin (red) and anti-GFP (green) stained caudal fin vascular plexus of 11dpf *Tg(fli1a:LIFEACT-clover)sh467*$^{/+}$ (**wt**) (n=15 fish), 13dpf *ift54*^{tp49}; *Tg(ubi:loxP-ift54-loxP-myr-mcherry,myl7:EGFP)sh488*$^{/+}$;*Tg(fli1a:LIFEACT-clover)sh467*$^{/+}$ (***ift54-/-; ubi:*ift54**) (n=4 fish) and 13dpf *ift54*^{tp49}; *Tg(ubi:loxP-ift54-loxP-myr-mcherry,myl7:EGFP)sh488*$^{/+}$*;Tg(kdrl:cre)s898*$^{/+}$;*Tg(fli1a:LIFEACT-clover)sh467*$^{/+}$ (***ift54-/-;ubi:ift54;kdrl:cre***) (n=4 fish). Slices at a **shallow** and **deep** level are shown along with orthogonal views resliced through the confocal stack at the level of cilia marked by **arrows**. Autofluorescent red blood cells (**R**) are visible in the vessel lumen. **Scale bar**, 10μm

Figure 8) Endothelial specific excision of the *Tg(ubi:loxP-ift54-loxP-myr-mcherry,myl7:EGFP)sh488* rescuing trangene causes no apparent further impairment to adult vasculature in *ift54*^{tp49}; *Tg(ubi:loxP-ift54-loxP-myr-mcherry,myl7:EGFP)sh488* fish. (A) Five month old *ift54*^{tp49}; *Tg(ubi:loxP-ift54-loxP-myr-mcherry,myl7:EGFP)sh488*$^{/+}$ (***ift54-/-;ubi:ift54***) (n=24) and *ift54*^{tp49}; *Tg(ubi:loxP-ift54-loxP-myr-mcherry,myl7:EGFP)sh488*$^{/+}$*; Tg(kdrl:cre)s898*$^{/+}$ (***ift54-/-;ubi:ift54;kdrl:cre***) fish (n=26). The *Tg(kdrl:cre)s898*$^{/+}$ caused no apparent further impairment to fish with partial transgenic rescue of *ift54*^{tp49}. **(B)** Confocal stack projections showing endothelial EGFP expression in flat mount views of swim bladder posterior chamber, pectoral fin and 4day-post-amputation regenerated caudal fin from sibling, four month old, *Tg(ubi:loxP-ift54-loxP-myr-mcherry,myl7:EGFP)sh488*$^{/+}$;*Tg(fli1a:EGFP)y1*$^{/+}$ (n=5) (**wt**) and *ift54*^{tp49}; *Tg(ubi:loxP-ift54-loxP-myr-mcherry,myl7:EGFP)sh488*$^{/+}$; *Tg(fli1a:EGFP)y1*$^{/+}$ (representative of

four animals analysed) (***ift54-/-;ubi:ift54***) and *ift54*^{tp49}; *Tg(ubi:loxP-ift54-loxP-myr-mcherry,myl7:EGFP)sh488*$^{/+}$*;Tg(kdrl:cre)s898*$^{/+}$; *Tg(fli1a:EGFP)y1*$^{/+}$ (n=5) (***ift54-/-;ubi:ift54;kdrl:cre***) fish. Yellow lines indicate approximate position of original fin amputation. **Scale bars**, 300μm

Figure 9) Endothelial specific excision of the *Tg(ubi:loxP-ift54-loxP-myr-mcherry,myl7:EGFP)sh488* rescuing trangene causes no apparent further impairment to adult retina vasculature in *ift54*^{tp49}; *Tg(ubi:loxP-ift54-loxP-myr-mcherry,myl7:EGFP)sh488* fish. Confocal stack projections showing endothelial EGFP expression in flat mount views of retina from sibling, four month old, *Tg(ubi:loxP-ift54-loxP-myr-mcherry,myl7:EGFP)sh488*$^{/+}$;*Tg(fli1a:EGFP)y1*$^{/+}$ (n=5) (**wt**) and *ift54*^{tp49}; *Tg(ubi:loxP-ift54-loxP-myr-mcherry,myl7:EGFP)sh488*$^{/+}$; *Tg(fli1a:EGFP)y1*$^{/+}$ (n=4) (***ift54-/-;ubi:ift54***) and *ift54*^{tp49}; *Tg(ubi:loxP-ift54-loxP-myr-mcherry,myl7:EGFP)sh488*$^{/+}$*;Tg(kdrl:cre)s898*$^{/+}$; *Tg(fli1a:EGFP)y1*$^{/+}$ (n=5) (***ift54-/-;ubi:ift54;kdrl:cre***) fish. The yellow boxes indicate the region of retina enlarged below. The *Tg(kdrl:cre)s898*$^{/+}$ caused no apparent further impairment to the vasculature in the fish with partial transgenic rescue of *ift54*^{tp49}. **Scale bars**, 300μm

Figure 10) Endothelial specific excision of the *Tg(ubi:loxP-ift54-loxP-myr-mcherry,myl7:EGFP)sh488* rescuing transgene causes no apparent further impairment to *tagln* expressing perivascular mural cells in *ift54*^{tp49}; *Tg(ubi:loxP-ift54-loxP-myr-mcherry,myl7:EGFP)sh488* fish (A) In situ hybridization for *tagln* expression on transverse posterior trunk frozen sections of 13dpf wt (**wt**) and sibling *ift54*^{tp49}; *Tg(ubi:loxP-ift54-loxP-myr-mcherry,myl7:EGFP)sh488*$^{/+}$ (***ift54-/-;ubi:ift54***) and *ift54*^{tp49}; *Tg(ubi:loxP-ift54-loxP-*

myr-mcherry,myl7:EGFP)sh488$^{/+}$*; Tg(kdrl:cre)s898*$^{/+}$ (***ift54-/-;ubi:ift54;kdrl:cre***) fish. The red line, in the cartoon below, illustrates where sections were taken. *tagln* expression is detected at the site of arteries such as the dorsal aorta (arrow). The *Tg(kdrl:cre)s898*$^{/+}$ caused no apparent further impairment to perivascular mural cells in the fish with partial transgenic rescue of *ift54*^{tp49}. Images representative of four animals analysed for each genotype. **(B)** In situ hybridization for *tagln* expression on transverse caudal fin frozen sections of adult wt (**wt**) and sibling *ift54*^{tp49}; *Tg(ubi:loxP-ift54-loxP-myr-mcherry,myl7:EGFP)sh488*$^{/+}$ (***ift54-;ubi:ift54***) and *ift54*^{tp49}; *Tg(ubi:loxP-ift54-loxP-myr-mcherry,myl7:EGFP)sh488*$^{/+}$*; Tg(kdrl:cre)s898*$^{/+}$ (***ift54-;ubi:ift54;kdrl:cre***) fish. The red line in the cartoon illustrates where sections were taken. The *Tg(kdrl:cre)s898*$^{/+}$ caused no apparent further impairment to *tagln* expression in the fish with partial transgenic rescue of *ift54*^{tp49}. Images representative of four animals analysed for each genotype.

Figure 11) Endothelial specific excision of the *Tg(ubi:loxP-ift54-loxP-myr-mcherry,myl7:EGFP)sh488* rescuing transgene causes no apparent further impairment to *tagln* expressing perivascular mural cells in *ift54*^{tp49}; *Tg(ubi:loxP-ift54-loxP-myr-mcherry,myl7:EGFP)sh488* fish expressing a *Tg(tagln:mcherry)sh441* transgene (A) Confocal stack projections showing mcherry fluorescence from 14dpf caudal fins of *Tg(tagln:mcherry)sh441*$^{/+}$ (***tagln:mcherry***), *Tg(ubi:loxP-ift54-loxP-myr-mcherry,myl7:EGFP)sh488*$^{/+}$*;Tg(kdrl:cre)s898* (***ubi:ift54;kdrl:cre***), and the control background fluorescence signal from unrecombined sibling *Tg(ubi:loxP-ift54-loxP-myr-mcherry,myl7:EGFP)sh488*$^{/+}$ (***ubi:ift54***) fish. Also shown are binary threshold processed images as used for quantification of the area of *Tg(tagln:mcherry)sh441*$^{/+}$

expression. Single focal plane transmitted light views are shown for orientation. The microscope settings suitable for *Tg(tagln:mcherry)sh441*$^{/+}$ detect insignificant fluorescence from *Tg(ubi:loxP-ift54-loxP-myr-mcherry,myl7:EGFP)sh488*$^{/+}$*;Tg(kdrl:cre)s898* but endothelial mcherry is detected at increased laser power. **Scale bar** 100μm. **(B)** Chart showing % of field of view with >threshold mcherry expression as measured from processed confocal projections of caudal fins from fish with the different transgenes as shown in representative examples in (**A**). Overlay shows median and interquartile range.

Figure 12) Endothelial specific excision of the *Tg(ubi:loxP-ift54-loxP-myr-mcherry,myl7:EGFP)sh488* rescuing transgene causes no apparent further impairment to perivascular mural cells in the caudal fin vascular plexus of *ift54*^{tp49}; *Tg(ubi:loxP-ift54-loxP-myr-mcherry,myl7:EGFP)sh488* fish.

(A) Confocal stack projections showing mcherry fluorescence from 17dpf caudal fins of *ift54*^{tp4}*; Tg(ubi:loxP-ift54-loxP-myr-mcherry,myl7:EGFP)sh488*$^{/+}$*; Tg(tagln:mcherry)sh441*$^{/+}$ (***ift54-/-; ubi:ift54; tagln:mcherry***), and *ift54*^{tp4}*; Tg(ubi:loxP-ift54-loxP-myr-mcherry,myl7:EGFP)sh488*$^{/+}$*;Tg(kdrl:cre)s898; Tg(tagln:mcherry)sh441*$^{/+}$ (***ift54-/-; ubi:ift54; tagln:mcherry; kdrl:cre***). Also shown are binary threshold processed images as used for quantification of the area of *Tg(tagln:mcherry)sh441*$^{/+}$ expression. Single focal plane transmitted light views are shown for orientation. **(B)** Chart shows % of field of view with >threshold mcherry expression as measured from processed confocal projections of caudal fins. Overlay shows median and interquartile range. Two-tailed Mann-Whitney test P=0.5362. The *Tg(kdrl:cre)s898*$^{/+}$ caused no apparent impairment to mural cell coverage in the newly developed fin vascular bed in the fish with partial transgenic rescue of *ift54*^{tp49}.

References

Baeyens N, Bandyopadhyay C, Coon BG, Yun S, Schwartz MA. 2016. Endothelial fluid shear stress sensing in vascular health and disease. J Clin Invest 126:821-828.

Ben J, Elworthy S, Ng AS, van Eeden F, Ingham PW. 2011. Targeted mutation of the talpid3 gene in zebrafish reveals its conserved requirement for ciliogenesis and Hedgehog signalling across the vertebrates. Development 138:4969-4978.

Bertrand JY, Chi NC, Santoso B, Teng S, Stainier DY, Traver D. 2010. Haematopoietic stem cells derive directly from aortic endothelium during development. Nature 464:108-111.

Borovina A, Superina S, Voskas D, Ciruna B. 2010. Vangl2 directs the posterior tilting and asymmetric localization of motile primary cilia. Nat Cell Biol 12:407-412.

Braissant OaW, W. 1998. A simplified in situ hybridization protocol using non-radioactively labeled probes to detect abundant and rare mRNAs on tissue sections. Biochemica 1:10-16.

Brown JM, Marsala C, Kosoy R, Gaertig J. 1999. Kinesin-II is preferentially targeted to assembling cilia and is required for ciliogenesis and normal cytokinesis in Tetrahymena. Mol Biol Cell 10:3081-3096.

Chen X, Gays D, Milia C, Santoro MM. 2017. Cilia Control Vascular Mural Cell Recruitment in Vertebrates. Cell Rep 18:1033-1047.

Dinsmore C, Reiter JF. 2016. Endothelial primary cilia inhibit atherosclerosis. EMBO Rep 17:156-166.

Drummond I. 2009. Studying cilia in zebrafish. Methods Cell Biol 93:197-217.

Eisa-Beygi S, Benslimane FM, El-Rass S, Prabhudesai S, Abdelrasoul MKA, Simpson PM, Yalcin HC, Burrows PE, Ramchandran R. 2018. Characterization of

Endothelial Cilia Distribution During Cerebral-Vascular Development in Zebrafish (Danio rerio). Arterioscler Thromb Vasc Biol 38:2806-2818.

Garcia-Cardena G, Slegtenhorst BR. 2016. Hemodynamic Control of Endothelial Cell Fates in Development. Annu Rev Cell Dev Biol 32:633-648.

Goetz JG, Steed E, Ferreira RR, Roth S, Ramspacher C, Boselli F, Charvin G, Liebling M, Wyart C, Schwab Y, Vermot J. 2014. Endothelial cilia mediate low flow sensing during zebrafish vascular development. Cell Rep 6:799-808.

Goetz SC, Anderson KV. 2010. The primary cilium: a signalling centre during vertebrate development. Nat Rev Genet 11:331-344.

Grimes DT, Boswell CW, Morante NF, Henkelman RM, Burdine RD, Ciruna B. 2016. Zebrafish models of idiopathic scoliosis link cerebrospinal fluid flow defects to spine curvature. Science 352:1341-1344.

Han YG, Kwok BH, Kernan MJ. 2003. Intraflagellar transport is required in Drosophila to differentiate sensory cilia but not sperm. Curr Biol 13:1679-1686.

Horstick EJ, Jordan DC, Bergeron SA, Tabor KM, Serpe M, Feldman B, Burgess HA. 2015. Increased functional protein expression using nucleotide sequence features enriched in highly expressed genes in zebrafish. Nucleic Acids Res 43:e48.

Hoshijima K, Jurynec MJ, Grunwald DJ. 2016. Precise Editing of the Zebrafish Genome Made Simple and Efficient. Dev Cell 36:654-667.

Huang CC, Lawson ND, Weinstein BM, Johnson SL. 2003a. reg6 is required for branching morphogenesis during blood vessel regeneration in zebrafish caudal fins. Dev Biol 264:263-274.

Huang CJ, Tu CT, Hsiao CD, Hsieh FJ, Tsai HJ. 2003b. Germ-line transmission of a myocardium-specific GFP transgene reveals critical regulatory elements in the cardiac myosin light chain 2 promoter of zebrafish. Dev Dyn 228:30-40.

Huang P, Schier AF. 2009. Dampened Hedgehog signaling but normal Wnt signaling in zebrafish without cilia. Development 136:3089-3098.

Huangfu D, Liu A, Rakeman AS, Murcia NS, Niswander L, Anderson KV. 2003. Hedgehog signalling in the mouse requires intraflagellar transport proteins. Nature 426:83-87.

Iomini C, Tejada K, Mo W, Vaananen H, Piperno G. 2004. Primary cilia of human endothelial cells disassemble under laminar shear stress. J Cell Biol 164:811-817.

Jones EA, le Noble F, Eichmann A. 2006. What determines blood vessel structure? Genetic prespecification vs. hemodynamics. Physiology (Bethesda) 21:388-395.

Kallakuri S, Yu JA, Li J, Li Y, Weinstein BM, Nicoli S, Sun Z. 2015. Endothelial cilia are essential for developmental vascular integrity in zebrafish. J Am Soc Nephrol 26:864-875.

Kramer-Zucker AG, Olale F, Haycraft CJ, Yoder BK, Schier AF, Drummond IA. 2005. Cilia-driven fluid flow in the zebrafish pronephros, brain and Kupffer's vesicle is required for normal organogenesis. Development 132:1907-1921.

Kwan KM, Fujimoto E, Grabher C, Mangum BD, Hardy ME, Campbell DS, Parant JM, Yost HJ, Kanki JP, Chien CB. 2007. The Tol2kit: a multisite gateway-based construction kit for Tol2 transposon transgenesis constructs. Dev Dyn 236:3088-3099.

Lamont RE, Vu W, Carter AD, Serluca FC, MacRae CA, Childs SJ. 2010. Hedgehog signaling via angiopoietin1 is required for developmental vascular stability. Mech Dev 127:159-168.

Lawson ND, Weinstein BM. 2002. In vivo imaging of embryonic vascular development using transgenic zebrafish. Dev Biol 248:307-318.

Leventea E, Hazime K, Zhao C, Malicki J. 2016. Analysis of cilia structure and function in zebrafish. Methods Cell Biol 133:179-227.

Lister JA, Robertson CP, Lepage T, Johnson SL, Raible DW. 1999. nacre encodes a zebrafish microphthalmia-related protein that regulates neural-crest-derived pigment cell fate. Development 126:3757-3767.

Liu Y, Zhu Z, Ho IHT, Shi Y, Xie Y, Li J, Zhang Y, Chan MTV, Cheng CHK. 2017. Germline-specific dgcr8 knockout in zebrafish using a BACK approach. Cell Mol Life Sci 74:2503-2511.

Malicki J, Avidor-Reiss T. 2014. From the cytoplasm into the cilium: bon voyage. Organogenesis 10:138-157.

Malicki J, Neuhauss SC, Schier AF, Solnica-Krezel L, Stemple DL, Stainier DY, Abdelilah S, Zwartkruis F, Rangini Z, Driever W. 1996. Mutations affecting development of the zebrafish retina. Development 123:263-273.

Malicki JJ, Johnson CA. 2017. The Cilium: Cellular Antenna and Central Processing Unit. Trends Cell Biol 27:126-140.

Mosimann C, Kaufman CK, Li P, Pugach EK, Tamplin OJ, Zon LI. 2011. Ubiquitous transgene expression and Cre-based recombination driven by the ubiquitin promoter in zebrafish. Development 138:169-177.

Nachury MV. 2014. How do cilia organize signalling cascades? Philos Trans R Soc Lond B Biol Sci 369.

Oh EC, Katsanis N. 2012. Cilia in vertebrate development and disease. Development 139:443-448.

Omori Y, Zhao C, Saras A, Mukhopadhyay S, Kim W, Furukawa T, Sengupta P, Veraksa A, Malicki J. 2008. Elipsa is an early determinant of ciliogenesis that links the IFT particle to membrane-associated small GTPase Rab8. Nat Cell Biol 10:437-444.

Parichy DM, Elizondo MR, Mills MG, Gordon TN, Engeszer RE. 2009. Normal table of postembryonic zebrafish development: staging by externally visible anatomy of the living fish. Dev Dyn 238:2975-3015.

Pazour GJ, Dickert BL, Vucica Y, Seeley ES, Rosenbaum JL, Witman GB, Cole DG. 2000. Chlamydomonas IFT88 and its mouse homologue, polycystic kidney disease gene tg737, are required for assembly of cilia and flagella. J Cell Biol 151:709-718.

Pooranachandran N, Malicki JJ. 2016. Unexpected Roles for Ciliary Kinesins and Intraflagellar Transport Proteins. Genetics 203:771-785.

Potente M, Gerhardt H, Carmeliet P. 2011. Basic and therapeutic aspects of angiogenesis. Cell 146:873-887.

Reiten I, Uslu FE, Fore S, Pelgrims R, Ringers C, Diaz Verdugo C, Hoffman M, Lal P, Kawakami K, Pekkan K, Yaksi E, Jurisch-Yaksi N. 2017. Motile-Cilia-Mediated Flow Improves Sensitivity and Temporal Resolution of Olfactory Computations. Curr Biol 27:166-174.

Reiter JF, Leroux MR. 2017. Genes and molecular pathways underpinning ciliopathies. Nat Rev Mol Cell Biol 18:533-547.

Riedl J, Crevenna AH, Kessenbrock K, Yu JH, Neukirchen D, Bista M, Bradke F, Jenne D, Holak TA, Werb Z, Sixt M, Wedlich-Soldner R. 2008. Lifeact: a versatile marker to visualize F-actin. Nat Methods 5:605-607.

Robertson GN, McGee CA, Dumbarton TC, Croll RP, Smith FM. 2007. Development of the swimbladder and its innervation in the zebrafish, Danio rerio. J Morphol 268:967-985.

Santoro MM, Pesce G, Stainier DY. 2009. Characterization of vascular mural cells during zebrafish development. Mech Dev 126:638-649.

Savage AM, Kurusamy S, Chen Y, Jiang Z, Chhabria K, MacDonald RB, Kim HR, Wilson HL, van Eeden FJM, Armesilla AL, Chico TJA, Wilkinson RN. 2019. tmem33 is essential for VEGF-mediated endothelial calcium oscillations and angiogenesis. Nat Commun 10:732.

Seiler C, Abrams J, Pack M. 2010. Characterization of zebrafish intestinal smooth muscle development using a novel sm22alpha-b promoter. Dev Dyn 239:2806-2812.

Sugimoto K, Hui SP, Sheng DZ, Kikuchi K. 2017. Dissection of zebrafish shha function using site-specific targeting with a Cre-dependent genetic switch. Elife 6.

Sun Z, Amsterdam A, Pazour GJ, Cole DG, Miller MS, Hopkins N. 2004. A genetic screen in zebrafish identifies cilia genes as a principal cause of cystic kidney. Development 131:4085-4093.

Tsujikawa M, Malicki J. 2004. Intraflagellar transport genes are essential for differentiation and survival of vertebrate sensory neurons. Neuron 42:703-716.

Vion AC, Alt S, Klaus-Bergmann A, Szymborska A, Zheng T, Perovic T, Hammoutene A, Oliveira MB, Bartels-Klein E, Hollfinger I, Rautou PE, Bernabeu MO, Gerhardt H. 2018. Primary cilia sensitize endothelial cells to BMP and prevent excessive vascular regression. J Cell Biol.

Wiggenhauser LM, Kohl K, Dietrich N, Hammes HP, Kroll J. 2017. Studying Diabetes Through the Eyes of a Fish: Microdissection, Visualization, and Analysis of the Adult tg(fli:EGFP) Zebrafish Retinal Vasculature. J Vis Exp.

Zhao C, Omori Y, Brodowska K, Kovach P, Malicki J. 2012. Kinesin-2 family in vertebrate ciliogenesis. Proc Natl Acad Sci U S A 109:2388-2393.

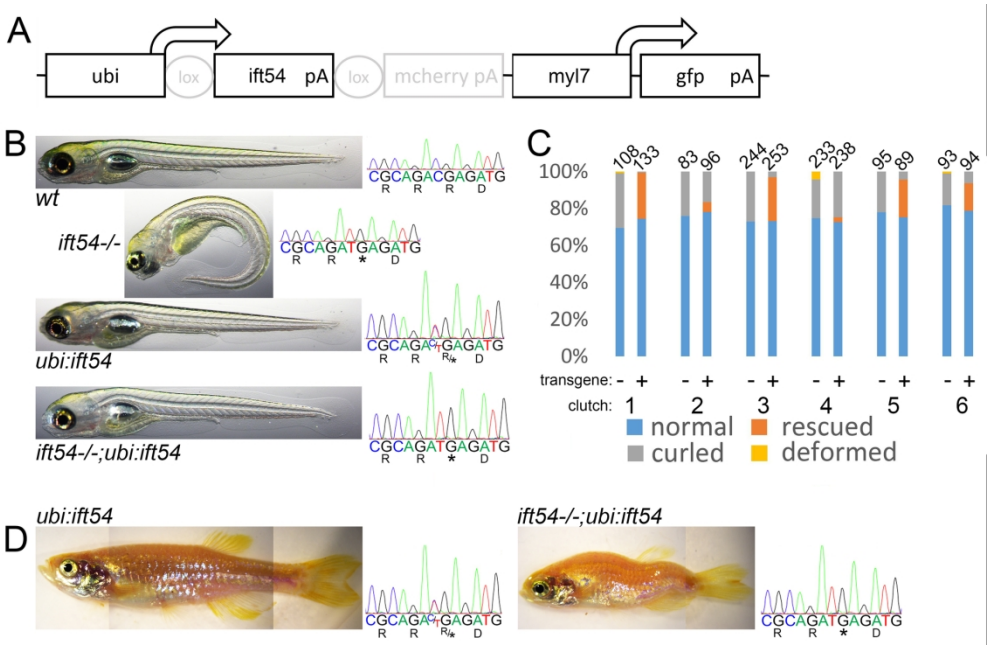

Figure 1

175x112mm (300 x 300 DPI)

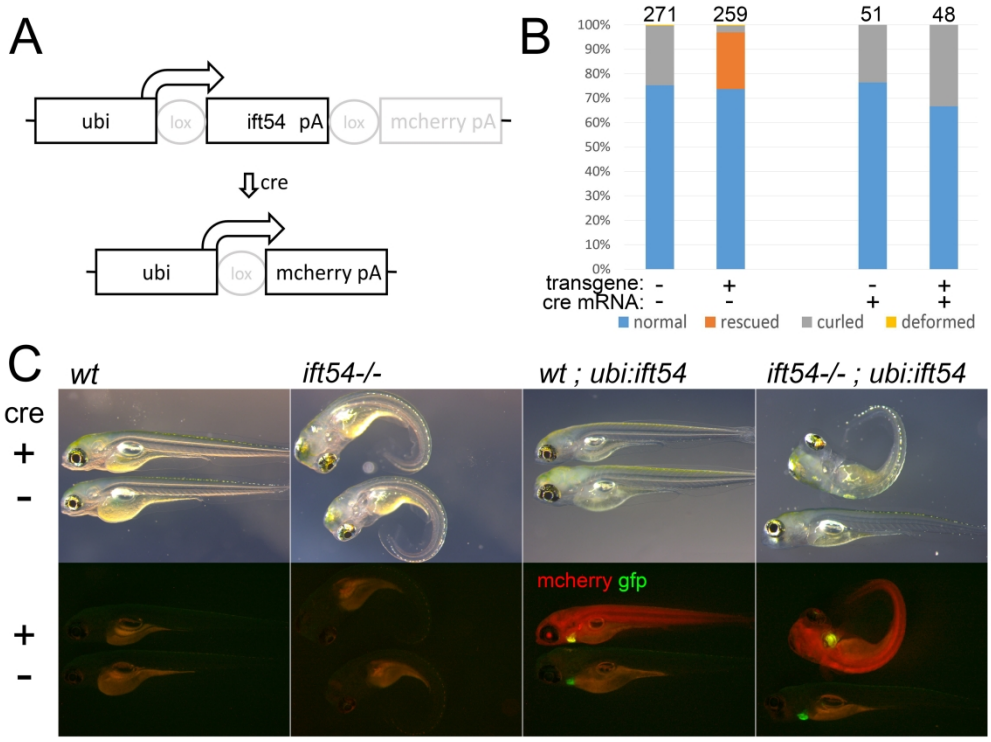

Figure 2

175x130mm (600 x 600 DPI)

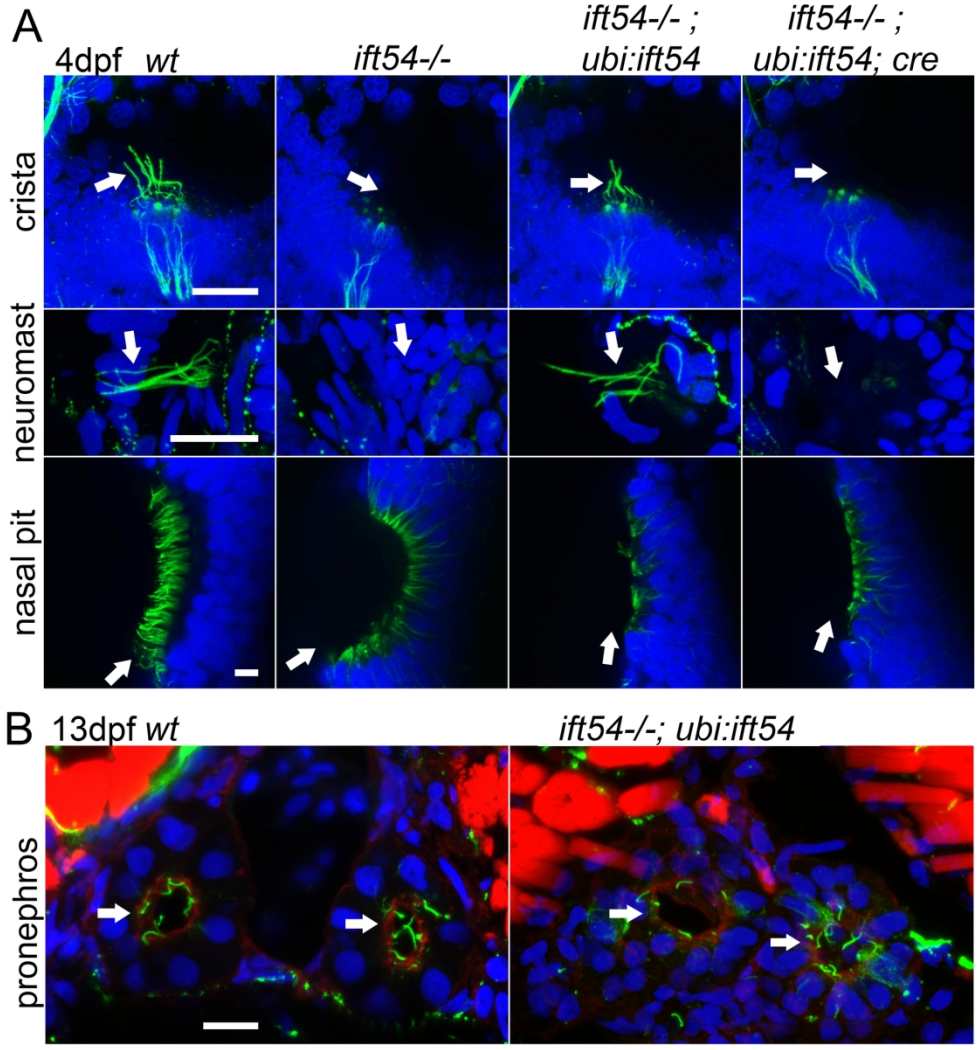

Figure 3

175x191mm (300 x 300 DPI)

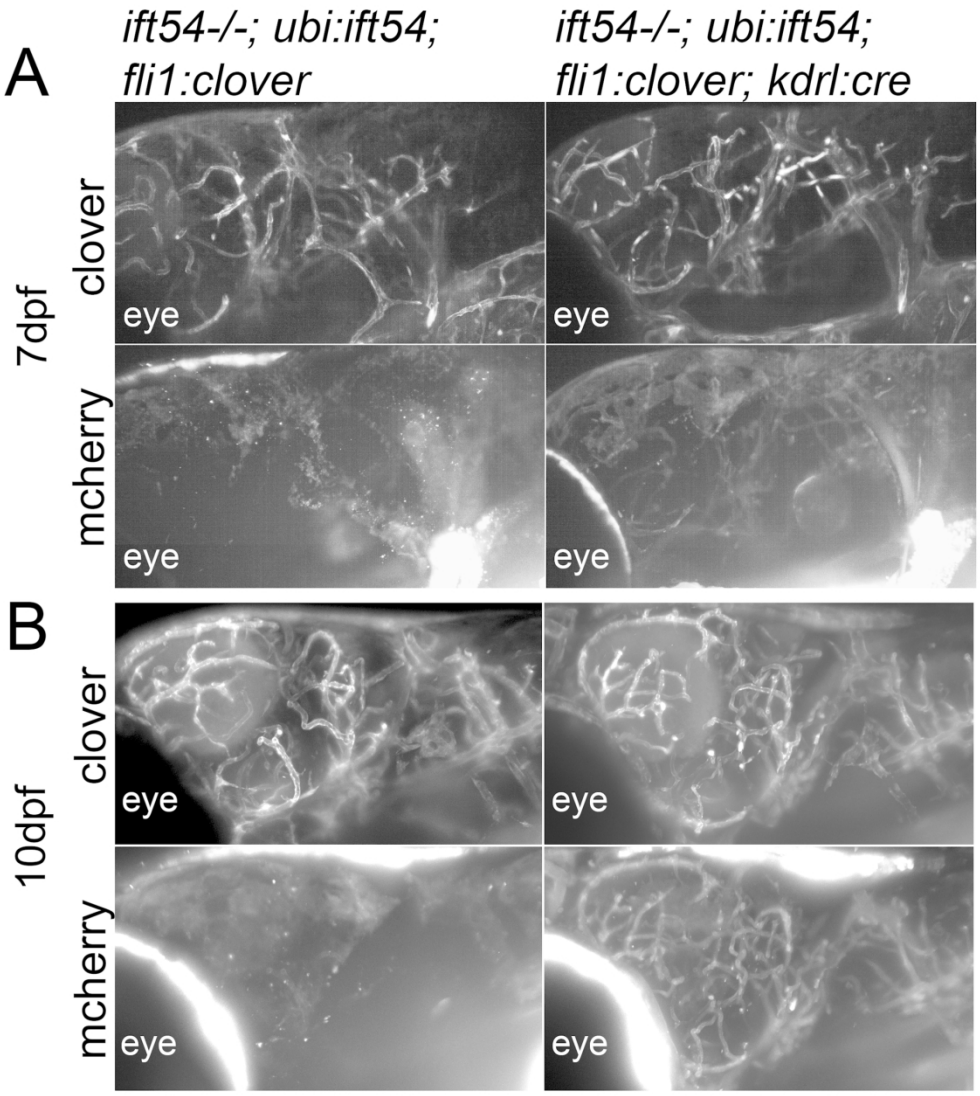

Figure 4

175x195mm (300 x 300 DPI)

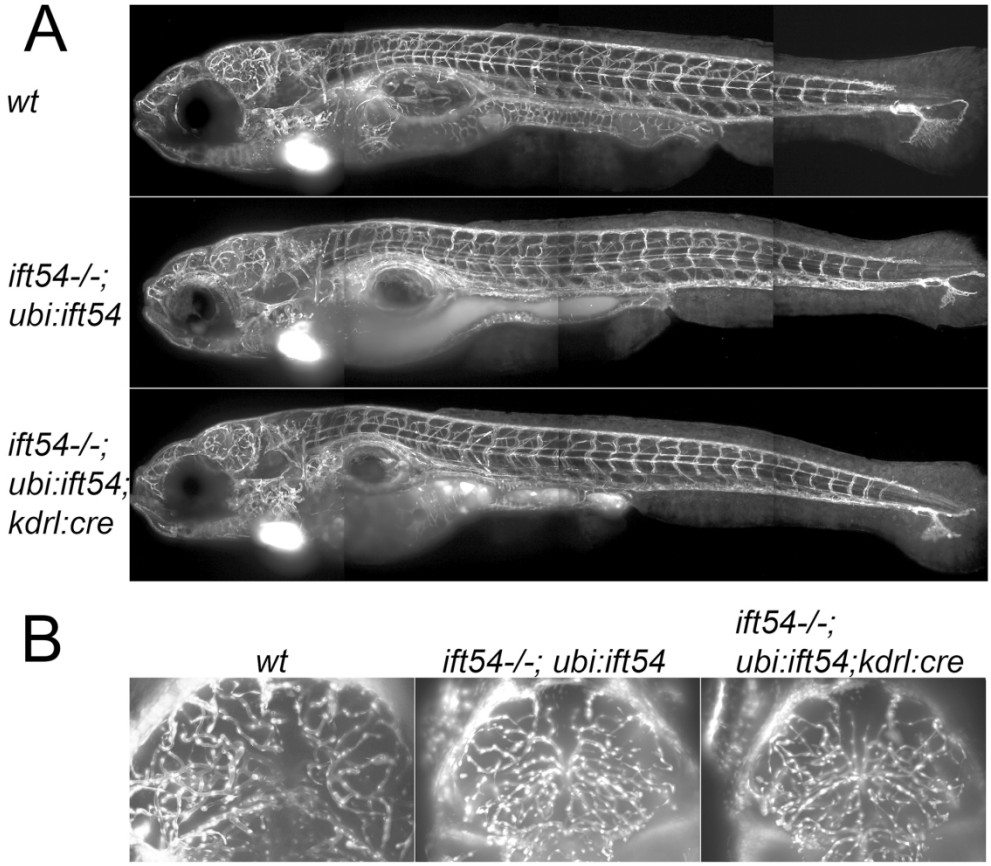

Figure 5

174x153mm (300 x 300 DPI)

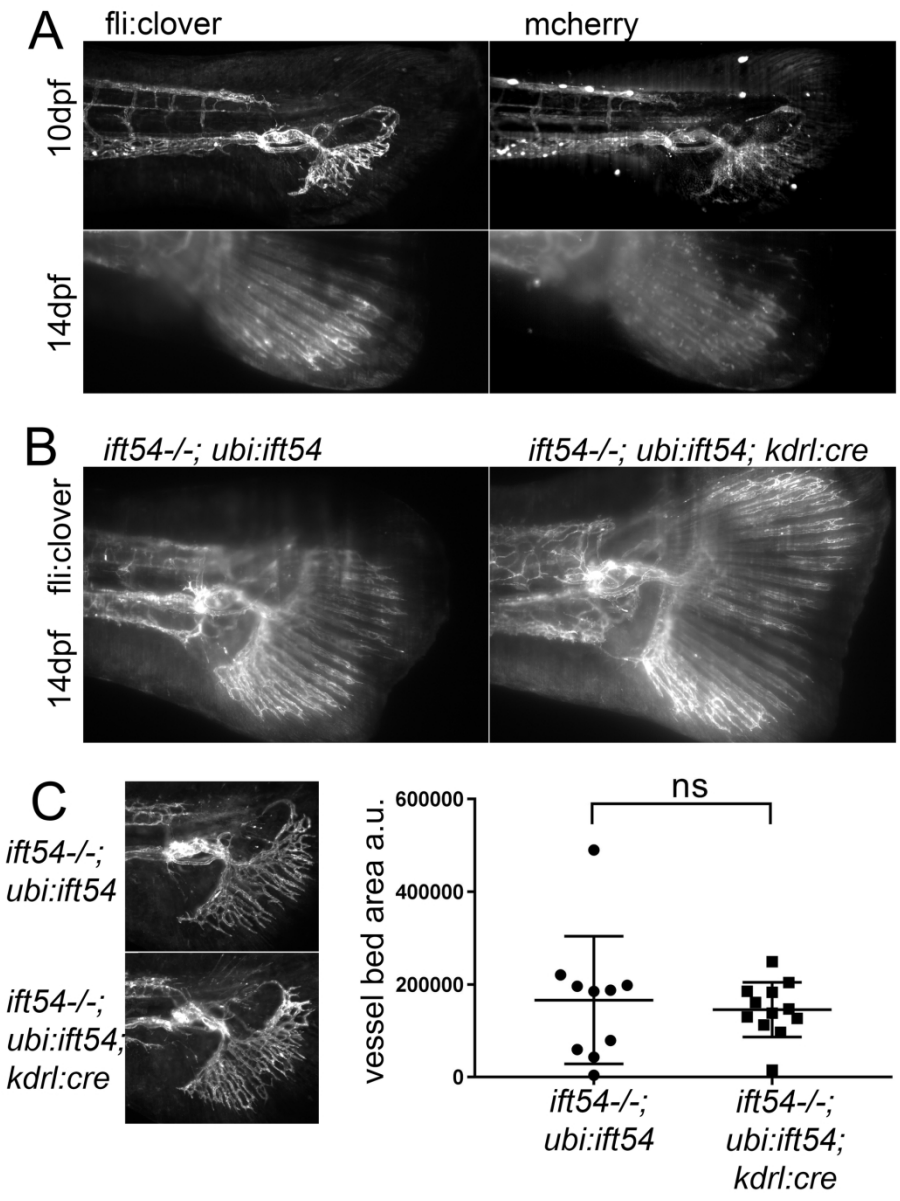

Figure 6

175x225mm (300 x 300 DPI)

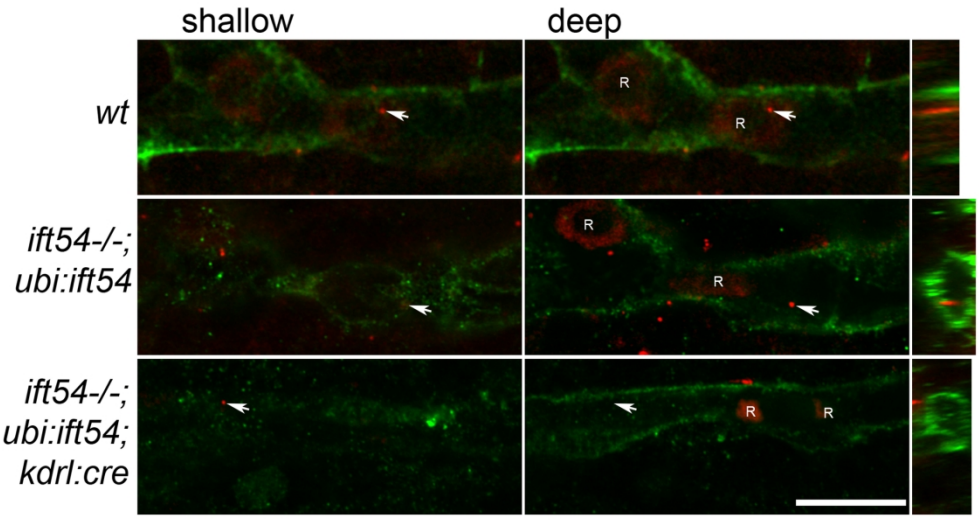

Figure 7

175x94mm (300 x 300 DPI)

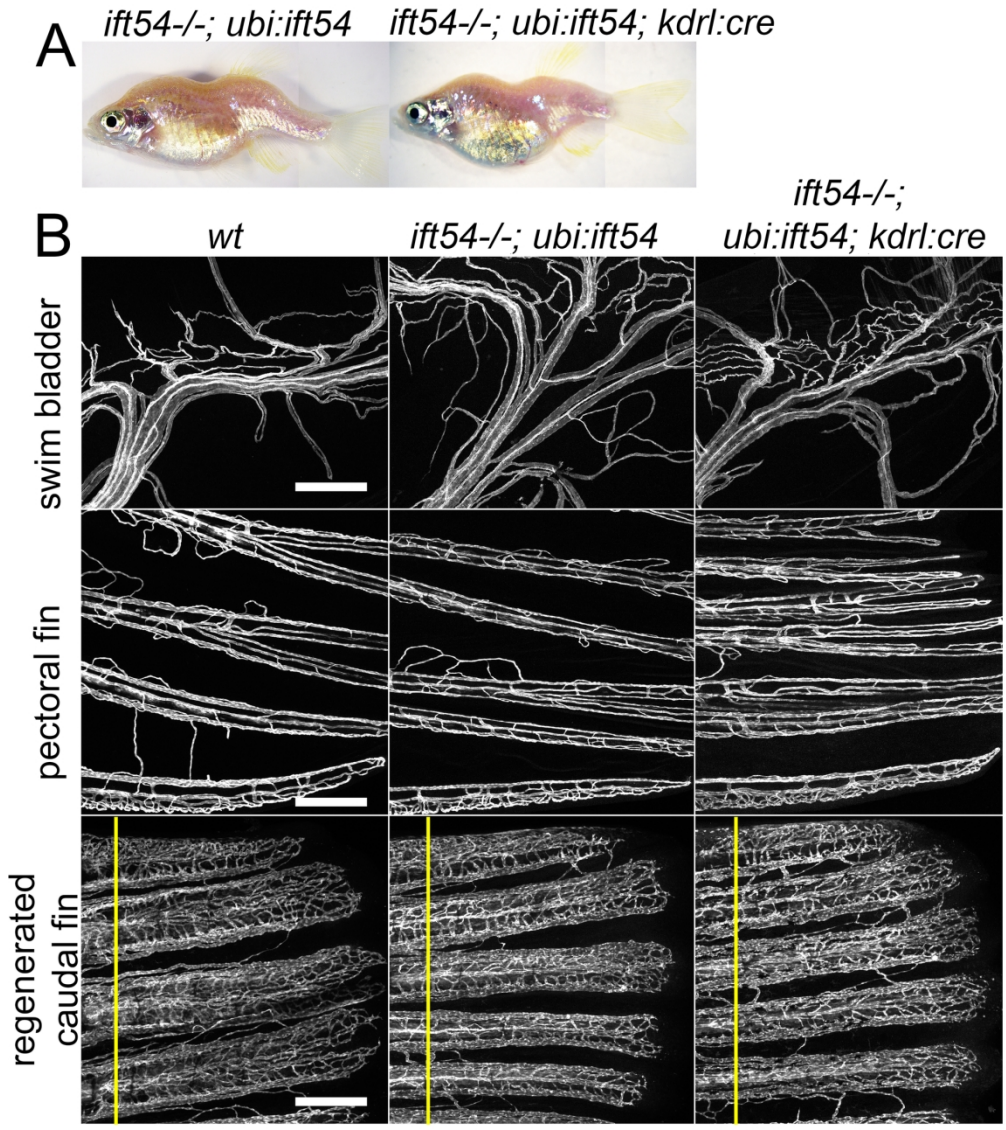

Figure 8

174x198mm (300 x 300 DPI)

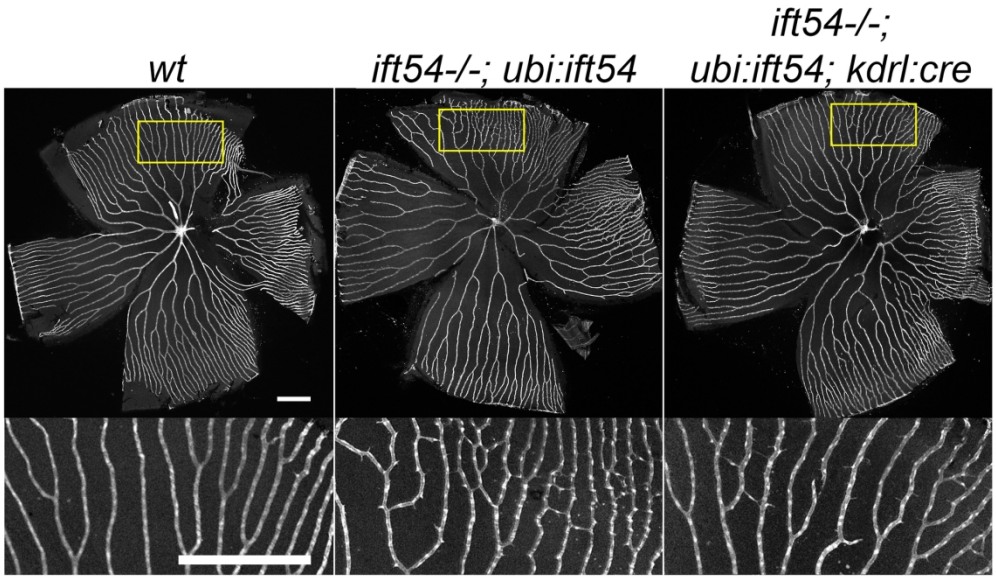

Figure 9

174x101mm (300 x 300 DPI)

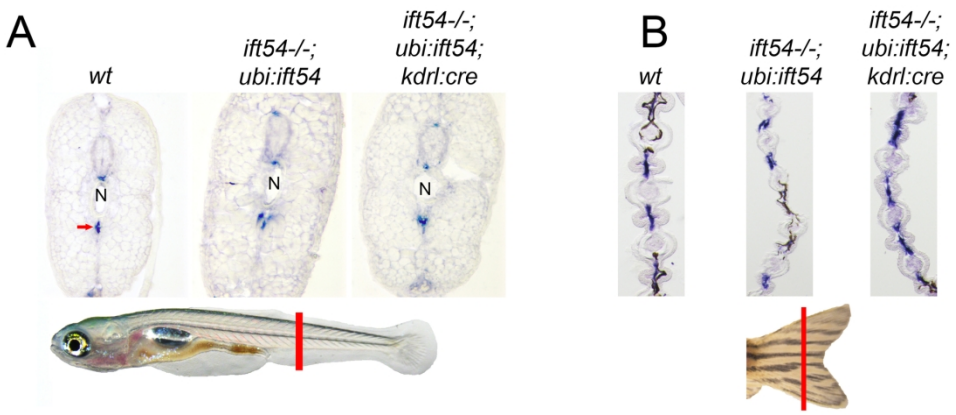

Figure 10

174x75mm (300 x 300 DPI)

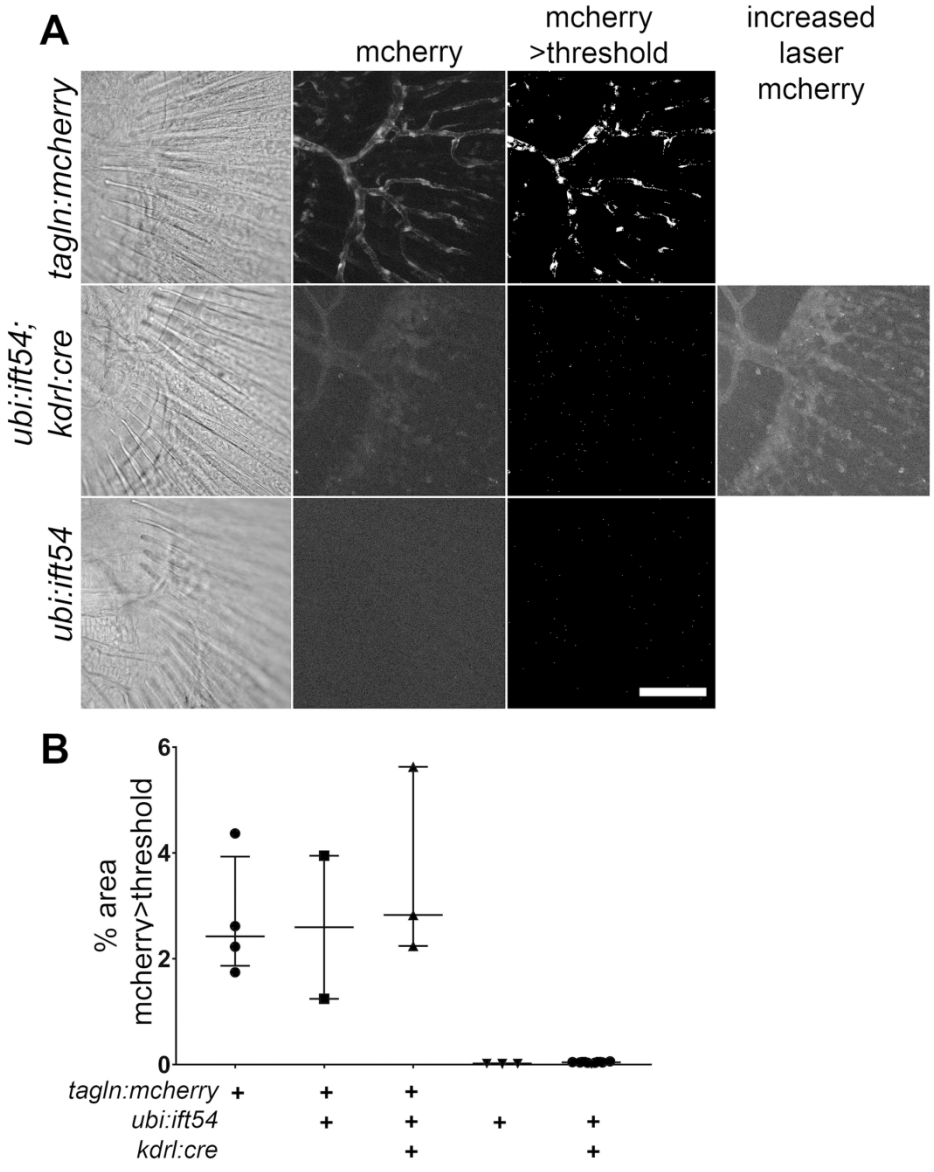

Figure 11

175x221mm (300 x 300 DPI)

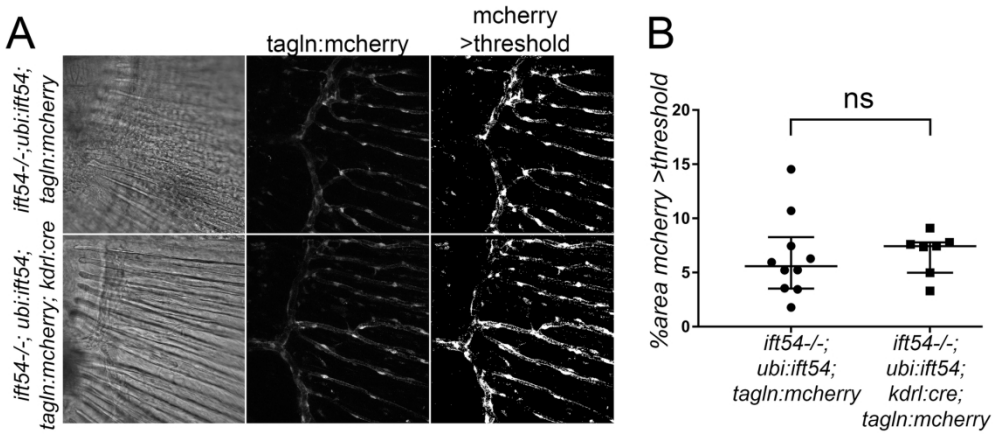

Figure 12

174x78mm (300 x 300 DPI)